UWB High Gain Antenna Array for SAR Based Breast Cancer Detection System

Mazhar Basyouni Tayel
Electrical Dep., Faculty of Engineering
Alexandria University
Alexandria, Egypt
e-mail: profbasyouni@gmail.com

Tamer Gaber Abouelnaga
Microstrip Circuits Dep., ERI
Communication Dep., HIET
Giza, Egypt
e-mail: tamer@eri.sci.eg

Asmaa Fereg Desouky
T. A, Communication Dep., HIET
Higher Institute of Engineering and Technology (HIET)
Kafer Elshiekh, Egypt
e-mail: asmaa.fereg@gmail.com

***Abstract*—Microwave breast cancer detection has become an attractive method for cancer early detection process. These systems uses directional and efficient antenna for transmitting and receiving signals. This paper is focused on the implementation of ultra-wideband, high gain, and directional microstrip antenna array for breast cancer detection system. Metamaterial cells are used for antenna gain enhancement purpose. Permeability and permittivity of metamaterial unit cell are obtained all over the operating bandwidth. Based on the metamaterial cell performance its geometry is altered to enhance the antenna gain at specific frequency band. Ultra wide band (UWB) unequal power divider is used to feed the proposed four elements antenna array based on Chebyshev excitation method. The proposed antenna has reasonable 3 dB beamwidth (3dBBW) and gain of 17.7 degrees and 14.5 dB at 4.12 GHz, respectively. The operating bandwidth (BW) which extends from 5.6 GHz to 10.9 GHz. The proposed antenna is fabricated, measured, and good agreement is obtained between simulated and measured results. Simulated specific absorption rate SAR is obtained and investigated for breast phantom where a small tumor is placed. The SAR results show clearly the tumor location in breast tissues which ensures the suitability of the proposed antenna array for cancer detection system.**

Keywords-breast cancer; metamaterial; SAR; antenna array; UWB

I. INTRODUCTION

Early detection of breast cancer make the treatment process more effective and easier. There are many methods for detection such as X-ray mammogram, ultrasound and MRI. X-ray mammogram uses ionizing radiation and requires painful compression for breast to have a good image [1]. Ultrasound and MRI methods are expensive [2], [3], [4]. Recently, UWB microwave system has become an attractive method for cancer detection and image reconstruction. UWB antenna is an important part of the UWB detection system. Many researchers have been discussed various UWB antenna structures. Table I shows many UWB antennas and compare among them.

TABLE I. COMPARISON BETWEEN UWB ANTENNAS

Ref.	Antenna size (mm^2)	BW (GHz)	Gain (dBi)	3dBBW (degree°)
[5]	23×29	4.5 – 10	5	Not reported
[6]	19×19	2 – 8	Not reported	80 °
[7]	30×30	0.5 – 2	6.3	78 °
[8]	42.8×42.8	3.1 – 10.6	5.5	Not reported
[9]	19.3×27.7	3.05 – 15	3.5	90 °
[10]	28×32	5.3 – 8.5	5	70 °
[11]	16×21	3.4 – 12.5	4.5	85 °
[12]	75×75	1.15 – 4.4	2.9	60 °

All the aforementioned researches suffer from the low gain value for single element antenna and wide 3dB beamwidth which are very important parameters for cancer detection system.

This paper introduces an ultra-wide band metamaterial antenna array with an effective breast cancer detection by using Specific Absorbed Rate (SAR). Firstly, single UWB antenna element with 16 metamaterial cells is designed and analyzed. Secondly, UWB unequal power divider is used to feed the antenna array based on Chebyshev elements excitation. 4 elements Chebyshev UWB antenna array with reflector is proposed. Finally, the proposed antenna array radiates a breast phantom with tumor and SAR result are investigated. The proposed antenna shows the possibility of detection process relies on SAR results. The metamaterial structure is chosen carefully for gain enhancement at narrow frequency band in the UWB of the proposed array. The metamaterial (MTML) unit cell and the antenna array are simulated using CST Microwave Studio 2014.

II. PROPOSED ANTENNA ARRAY DESIGN AND CONFIGURATION

In [13], a transition from coaxial-to-coplanar waveguide (CPW) was presented. This transition is important for avoiding air gap between antennas and patient's skin which may cause power losses. In this paper, this transition is used in developing an UWB antenna for detection process.

978-1-5386-6392-9/18/$31.00 ©2018 IEEE

Section A, B and C present the proposed antenna array structure stages.

A. Antenna Element

The proposed antenna structure is shown in Fig. 1a. It consists of the common coplanar fed slot antenna [14] as radiator and the proposed transition [13]. The FR4 dielectric constant of 4.6 and height 1.53 mm considered as antenna substrate. The substrate size of the radiator is 49 mm × 30 mm × 1.53 mm. Fig. 1b shows the proposed antenna optimized dimensions shown in Table II. Figure 2a shows the simulated return loss of the proposed antenna, extended from (3.6 GHz – 10 GHz). Figure 2b shows that a maximum gain of 4.5 dB is obtained at 8 GHz.

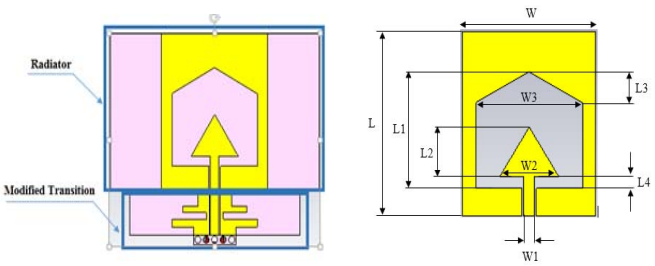

(a) (b)

Figure 1. (a) The proposed antenna structure (Transformation and radiator) and (b) The proposed antenna dimensions.

TABLE II. PROPOSED ANTENNA PARAMETERS VALUE IN MM

Parameter	W	W1	W2	W3	L	L1	L2	L3
Dimension (mm)	25	2.023	11	20	30	19	8	5

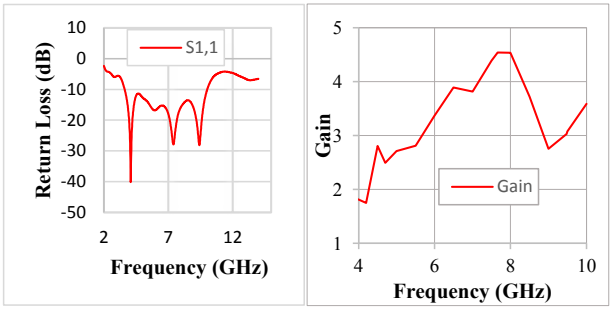

(a) (b)

Figure 2. (a) The simulated return loss of the proposed antenna (b) The simulated gain of the proposed antenna.

From Fig. 2b it is noticed that the gain of the proposed antenna has low values at maximum value of 4.5 dBi and has to be enhanced for detection process. To solve this problem, metamaterial cells are incorporated to improve the gain of the proposed antenna structure.

B. Antenna Element with Metamaterial Cells

1) Metamaterial cells

Metamaterial cell is an integration of a capacitive loaded strip (CLS), modified split ring resonator (SRR) and wire, to achieve a negative electrical permittivity and a negative magnetic permeability [9]. This results in a spectacular negative refractive index that enables amplification of the radiated power of the proposed antenna. A low-cost FR4 substrate material is used to design and print this proposed cell. The overall structure size is 10 mm × 7.29 mm × 1.53 mm. The metamaterial unit cell is based on an SRR structure. The SRR structure is made of two octagonal loops. A smaller octagonal loop with in a bigger octagonal one. The smaller one with gaps in the middle of the octagonal shape. These gaps make a capacitance which control the resonant characteristic of the metamaterial structure. The CLSs which act as electric dipole are I-shaped striplines that mimic long metallic wires. The combined structure (SRR and CLSs) allows for simultaneous electric and magnetic resonance because the SRR resonates with a perpendicular magnetic field and the CLSs resonates through a parallel electric field. Figure 3a shows the simulation geometry of the unit cell. The MTML unit cell is simulated using CST Microwave Studio. The structure used for testing was located between two waveguide ports situated on each side of the x-axis. An electromagnetic wave was excited along the x-axis. A perfectly conducting electrical boundary condition was applied along the walls perpendicular to the y- axis and a perfectly conducting magnetic boundary was applied to the walls perpendicular to z-axis. The normalized impedance is matched to 50 Ω. Figure 3b shows the octagonal metamaterial parameters.

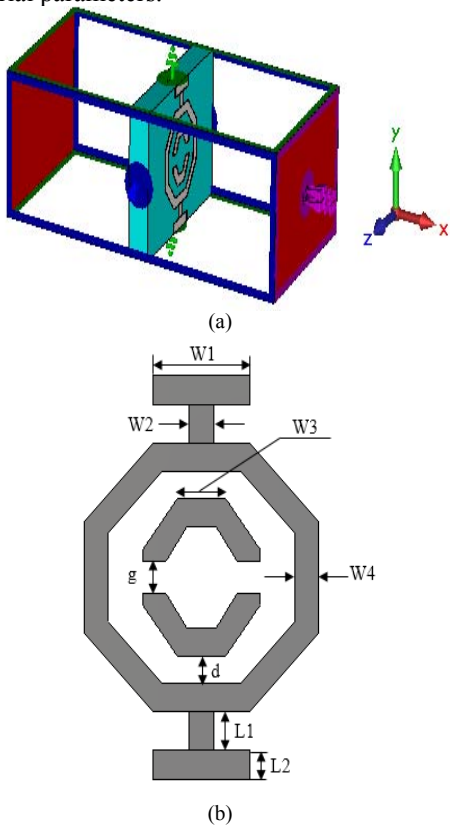

(a)

(b)

Figure 3. (a) The proposed structure of the MTML unit cell and (b) The proposed MTML structure specification.

TABLE III. THE DESIGN PARAMETERS OF THE PROPOSED UNIT CELL

Parameter	W1	W2	W3	W4	L1	L2	g	d
Dimension (mm)	2	0.5	1	0.5	0.7	0.52	0.6	0.5

Table III shows the value of the proposed MTML dimensions. The S-parameters are shown in Fig. 4. The Nicolson-Ross-Weir approach [15], [16] was used to extract the constitutive effective parameters from S_{11} and S_{21} including the relative permeability μ_r , the relative permittivity $\mathcal{E}_r$ and their refractive index n_r as follow

$$\mathcal{E}_r = \frac{2}{jk_o d} * \frac{1 - V_1}{1 + V_1} \quad (1)$$

$$\mu_r = \frac{2}{jk_o d} * \frac{1 - V_2}{1 + V_2} \quad (2)$$

$$n_r = \sqrt{\mathcal{E}_r \mu_r} \quad (3)$$

$$V_1 = S_{21} + S_{11} \quad (4)$$

$$V_2 = S_{21} - S_{11} \quad (5)$$

where: $k_o = \omega / C$, d = slab thickness and C = speed of light. A Matlab code is built to extract the relative permittivity $\mathcal{E}_r$ and relative permeability μ_r curves from the S-parameters. Figure 5 shows the proposed MTML permittivity $\mathcal{E}_r$ and permeability μ_r. Table IV shows the values of permittivity and permeability in the negative frequency zone.

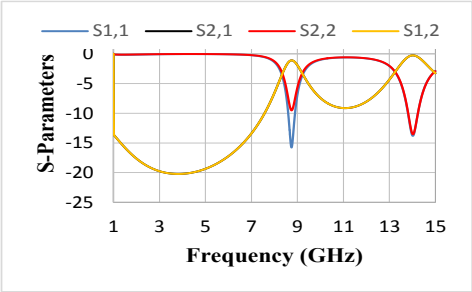

Figure 4. The magnitude of the S-parameters for the proposed MTML unit cell.

TABLE IV. NEGATIVE PERMEABILITY AND PERMITTIVITY IN THE FREQUENCY ZONE

Parameter	Negative Frequency Zone (GHz)
Permitivity, $\mathcal{E}_r$	1 – 6.5, 8.7–12.5
Permeability, μ_r	6.5 – 9, 9.2 – 12

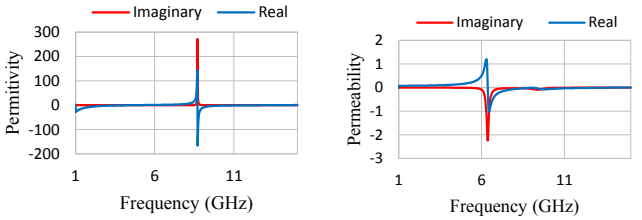

(a) (b)

Figure 5. The proposed unit cell (a) permittivity $\mathcal{E}_r$ and (b) permeability μ_r.

2) Antenna loaded with MTML

Figure 6a shows the antenna where sixteen MTML cells are placed along x and y-axis of the antenna substrate. These cells are in the direction of the antenna radiation to enhance the antenna directivity. The antenna is printed on FR4 material. The overall antenna dimensions are 49 mm × 38.7 mm × 1.53 mm.

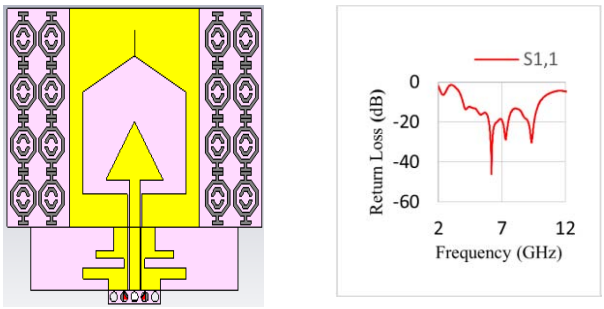

(a) (b)

Figure 6. (a) The proposed antenna with proposed MTML unit cell and (b) The simulated return loss of the proposed antenna with MTML.

Figure 6b shows the simulated return loss of the proposed antenna covering frequency band from (3.9 GHz – 10 GHz). Fig. 7 shows a comparison between the gain value of the proposed antenna with and without metamaterial cells. It is noticed that the incorporation of metamaterial cells shows a gain enhancement of about 2dB. Figure 8 shows the 3D radiation pattern of the antenna, one noticed that the antenna has an omnidirectional radiation pattern. Also, the beam width (angular width) is 70.3˚. Both results are not good enough for breast cancer early detection process. The goal is to have an antenna with a narrow 3 dB beamwidth .So, an antenna array will be used. Figure 9 shows the radiation pattern in x-z plane.

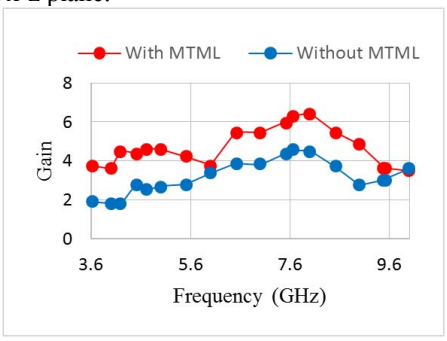

Figure 7. The gain values of the proposed antenna without metamaterial and with MTML.

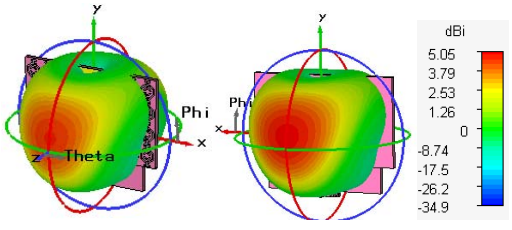

Figure 8. The radiation pattern of proposed antenna with metamaterial from front side and back side.

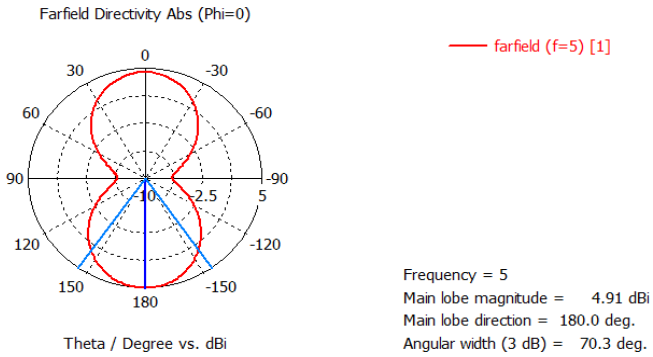

Figure 9. The radiation pattern in x-z plane.

C. *Antenna Array*

The proposed antenna element with metamaterial 16 cells is used to design a 4×1 antenna array. The proposed antenna array operate at UWB rang which extend from 5.6 GHz – 10.9 GHz. Resonant frequencies at 3.08 GHz, 4.12 GHz, and 5.16 GHz are occurred. Figure 10 shows the structure of the 4×1 antenna array with feeding network based on UWB Wilkinson unequal power divider which was presented in [17]. Figure 11 shows the fabricated antenna array where a reflector is placed at back side. The reflector size is 230 mm × 60 mm at 10 mm from the antenna substrate. The reflection coefficient of the fabricated antenna array and its simulated counterpart are shown in Fig. 12. Figure 13 shows comparison between the uniform linear array (ULA) gain without MTML and with MTML. One can notice that the incorporation of metamaterial cells shows a gain enhancement of about 3dB are obtained at frequency bands which extend from 9 GHz to 10.5 GHz and from 5.8 GHz to 8.5 GHz, respectively. 3D radiation pattern of the proposed antenna array is shown in Fig. 14 where directivity of 14.5 dBi is obtained at 4.12 GHz. Figure 15 shows the XZ plane of the radiation pattern where a side loop level of -11.2 dBi and half power beam width = 17.7˚ are obtained. Table V shows a comparison between antenna parameters of single element with metamaterial and 4 x 1 antenna array.

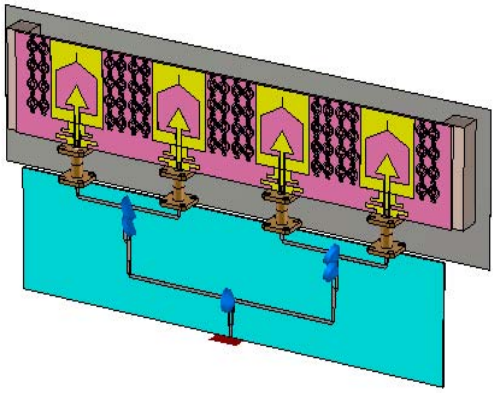

Figure 10. The structure of the 4×1 antenna array with feeding network based on λ/4 transformer.

(a) (b)

Figure 11. The fabricated antenna array (a) front side and (b) back side.

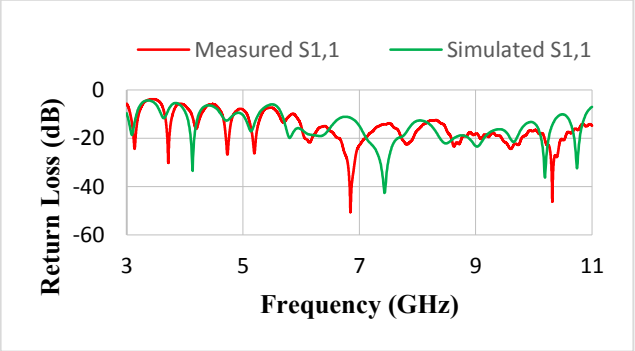

Figure 12. The reflection coefficient of the fabricated antenna array and simulated antenna array.

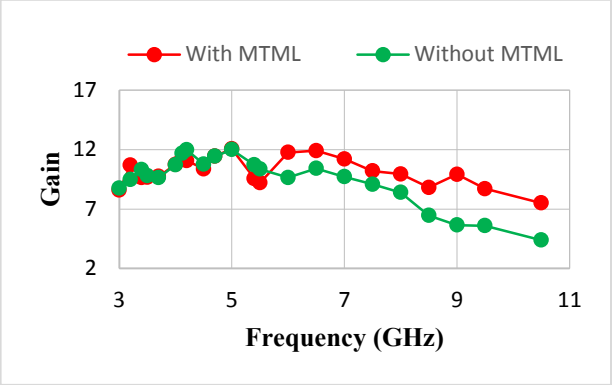

Figure 13. The gain values of the proposed antenna array without MTML and with MTML.

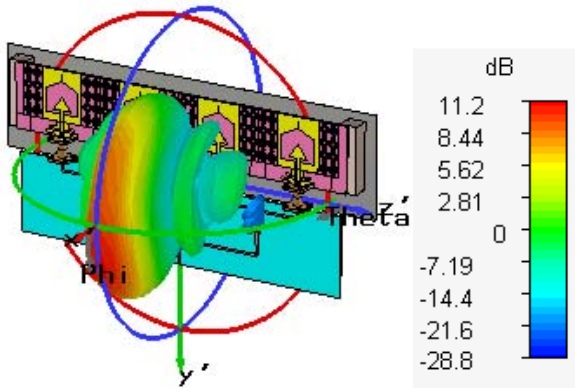

Figure 14. The 3D radiation pattern of the proposed antenna array.

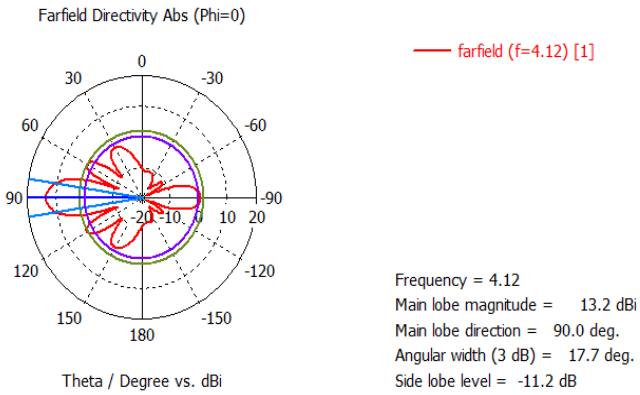

Figure 15. The XZ plane of the radiation pattern.

TABLE V. A COMPARISON OF ANTENNA PARAMETERS BETWEEN SINGLE ELEMENT OF ANTENNA, SINGLE ELEMENT WITH MTML AND ARRAY

	Resonance frequency	**Bandwidth GHz**	**Beam width**	**Gain dB**
Single element with MTML	6.1 GHz, 7.3 GHz, 9.3 GHz	(3.9 – 10)	56 degree at 6.1GHz 75.6 degree at 7.3 GHz 122 degree at 9.3 GHz	(3.6 - 6.5)
Array with MTML	4.12GHz, 6.4 GHz, 7.4GHz, 8.5GHz, 9.68GHz, 10.22GHz, 10.77GHz	(5.6 – 10.9)	17.7 degree at 4.12GHz 11.6 degree at 6.4GHz 9.6 degree at 7.4GHz 10.1 degree at 8.5GHz	(10 – 12)

III. ANTENNA ARRAY WITH BREAST PHANTOM

For detection process, a hemisphere breast phantom of radius 45 mm is built. The phantom consists of two layer tissues and tumor. The phantom is simulated to have a dielectric constant similar to the real dielectric constant of tissues and tumor. The dielectric constant of tissue layer $\mathcal{E}_r = 9$ and conductivity $\sigma = 0.4$ S/m and the dielectric constant of the tumor layer $\mathcal{E}_r = 50$ and conductivity $\sigma = 7$ S/m [18]. The breast phantom is illuminated with an UWB signal from the proposed antenna array. The maximum SAR is calculated on the phantom with tumor. The Specific Absorption Rate (SAR) is defined by using the following equation [1] , [19]

$$\text{SAR} = \frac{\sigma\,|E|^2}{\rho} \qquad (6)$$

where E is the rms electric field strength (V/m), σ is the conductivity of the material (S/m) and ρ is the mass density of the material (Kg/m^3). The maximum limit of SAR value assigned by Federal Communication Commission (FCC) in united states, which is 1.6 W/Kg averaged over 1 g volume, and the standard in Europe being 2 W/Kg averaged over 10 g volume [20]. In this paper, the spatial average of SAR of 1 g or 10 g volumetric sample is calculated over the breast phantom model along the UWB range of the proposed antenna array. Different tumor sizes are tested for early detection verification purpose. Table V shows the SAR distribution inside the phantom with tumor size of R=5 mm at different frequencies.

It is observed from Table VI that the maximum SAR values are higher in the tumor compared to the healthy tissues, but in some frequencies there are maximum values at the edges of the breast phantom this due to the transition from breast tissues to air. To solve this problem at the simulation, the edge of breast phantom can be extended much longer. Table VI shows that the values of maximum SAR are below the maximum limit assigned by Federal Communications Commission (FCC). These result shows a successful detection for malignant cells by using SAR. This method of detection has been used by Hikage and Okano [21], [22].

TABLE VI. THE SAR DISTRIBUTION INSIDE THE PHANTOM WITH TUMOR AT DIFFERENT FREQUENCIES

Frequency (GHz)	**SAR distribution**	**Maximum SAR value W/Kg (1g Standard)**
4.12	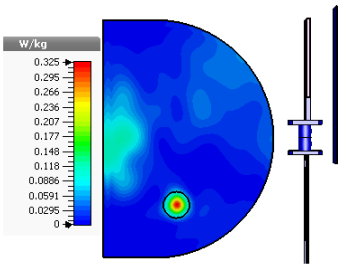	0.325
6	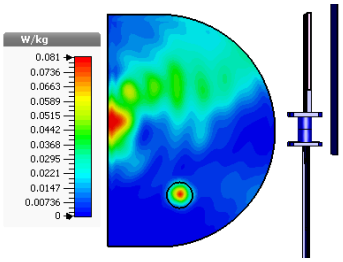	0.081
7	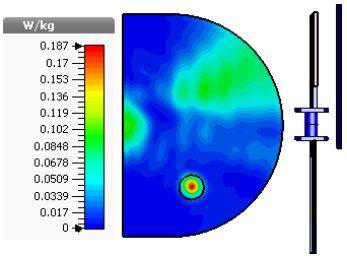	0.187

IV. CONCLUSION

A design and implementation of an UWB metamaterial antenna array was introduced for breast cancer early detection. The antenna array bandwidth extends from 5.6

GHz to 10.9 GHz. The introduction of metamaterial cells enhanced the gain of single element antenna of about 2dB. The proposed antenna array of 4×1 elements achieved high directivity, high gain and reasonable beam width at different frequency bands. A hemisphere breast phantom with 5mm tumor radius was tested at different frequencies for tumor detection process. SAR results were investigated using 1g standard and had shown that the highest SAR values were in the tumor compared to the healthy tissues. Good agreement was obtained between simulated and measured results.

REFERENCES

[1] E. C. Fear, P. M. Meaney, and M. a Stuchly, "Microwaves for Breast Cancer Detection?," IEEE Potentials, vol. 22, pp. 12, 2003.

[2] J. L. and R. B. R. Nilavalan, I.J. Craddock, A. Preece, "Wideband microstrip patch antenna design for breast cancer tumour detection," IET Microw. Antennas Propag., vol. 1, pp. 277–281, 2007.

[3] S. C. Hagness, A. Taflove, and J. E. Bridges, "Two-dimensional FDTD analysis of a pulsed microwave confocal system for breast cancer detection: Fixed-focus and antenna-array sensors," IEEE Trans. Biomed. Eng., vol. 45, pp. 1470–1479, 1998.

[4] E. C. Fear and M. A. Stuchly, "Microwave detection of breast cancer," IEEE Trans. Microw. Theory Tech., vol. 48, pp. 1854, 2000.

[5] M. Klemm, I. Craddock, J. Leendertz, A. Preece, and R. Benjamin, "Radar-based breast cancer detection using a hemispherical antenna array—experimental results," IEEE Trans. Antennas Propag., vol. 57, pp. 1692–1704, 2009.

[6] Y. Wang, A. E. Fathy, and M. R. Mahfouz, "Novel compact tapered microstrip slot antenna for microwave breast imaging," IEEE Antennas Propag. Soc. AP-S Int. Symp., pp. 2119–2122, 2011.

[7] X. Li, M. Jalilvand, Y. L. Sit, and T. Zwick, "A compact double-layer on-body matched bowtie antenna for medical diagnosis," IEEE Trans. Antennas Propag., vol. 62, pp. 1808–1816, 2014.

[8] M. H. Bah, J. Hong, D. A. Jamro, J. J. Liang, and E. A. Kponou, "Vivaldi antenna and breast phantom design for breast cancer imaging," IEEE conf., 7th International Conference on Biomedical Engineering and Informatics (BMEI), pp. 90–93, 2014.

[9] M. M. Islam, M. T. Islam, M. R. I. Faruque, M. Samsuzzaman, N. Misran, and H. Arshad, "Microwave imaging sensor using compact metamaterial UWB antenna with a high correlation factor," Materials (Basel)., vol. 8, pp. 4631–4651, 2015.

[10] L. W. Li, Y. N. Li, T. S. Yeo, J. R. Mosig, and O. J. F. Martin, "A broadband and high-gain metamaterial microstrip antenna," Appl. Phys. Lett., vol. 96, no. 16, 2010.

[11] M. M. Islam, M. T. Islam, M. Samsuzzaman, M. R. I. Faruque, N. Misran, and M. F. Mansor, "A miniaturized antenna with negative index metamaterial based on modified SRR and CLS unit cell for UWB microwave imaging applications," Materials (Basel)., vol. 8, pp. 392–407, 2015.

[12] B. Wu, Y. Ji, and G. Fang, "Design and measurement of compact tapered slot antenna for UWB microwave imaging radar," 2009 9th Int. Conf. Electron. Meas. Instruments, pp. 2-226-2–229, 2009.

[13] M. B. Tayel, T. G. Abouelnaga, and A. F. Desouky, "A Coaxial-to-CPW Transition for Microwave Breast Cancer Detection Antennas," IOSR J. Electr. Electron. Eng., vol. 11, pp. 42–53, 2016.

[14] K. C. Gupta, R. Garg, I. Bahl and P. Bhartia, Microstrip Lines and Slotlines, Second edition, Artech House Boston, London, 1996.s

[15] M. T. ariqul Islam, M. M. oinul Islam, M. Samsuzzaman, M. R. ashed I. Faruque, and N. Misran, "A Negative Index Metamaterial-Inspired UWB Antenna with an Integration of Complementary SRR and CLS Unit Cells for Microwave Imaging Sensor Applications," Sensors (Basel)., vol. 15, pp. 11601–11627, 2015.

[16] I. M. Rusni, A. Ismail, A. R. H. Alhawari, M. N. Hamidon, and N. A. Yusof, "An aligned-gap and centered-gap rectangular multiple split ring resonator for dielectric sensing applications," Sensors (Switzerland), vol. 14, pp. 13134–13148, 2014.

[17] O. Dardeer, T. Abouelnaga, A. Mohra, and H. Elhennawy, "Compact UWB Power Divider, Analysis and Design," J. Electromagn. Anal. Appl., vol. 9, pp. 9–21, 2017.

[18] S. C. Hagness, a. Taflove, and J. E. Bridges, "Three-dimensional FDTD analysis of an ultrawideband antenna-array\nelement for confocal microwave imaging of nonpalpable breast tumors," IEEE Antennas Propag. Soc. Int. Symp. 1999 Dig., vol. 3, pp. 1886–1889, 1999.

[19] I. Std, I. I. Committee, E. Safety "IEEE Recommended Practice for Measurements and Computations of Radio Frequency Electromagnetic Fields With Respect to Human Exposure to Such Fields , 100 kHz – 300 GHz", IEEE Std C95.3-2002 (Revision of IEEE Std C95.3-1991), 2002.

[20] A. G. Dagheyan, A. Molaei, R. Obermeier, and J. Martinez-Lorenzo, "Preliminary imaging results and SAR analysis of a microwave imaging system for early breast cancer detection," 2016 38th Annu. Int. Conf. IEEE Eng. Med. Biol. Soc., pp. 1066–1069, 2016.

[21] T. Hikage, Y. Kawamura, and T. Nojima, "Whole-body averaged SAR measurement method using cylindrical scanning of external electromagnetic fields," 2009 Int. Symp. Electromagn. Compat. - EMC Eur., 2009.

[22] Y. Okano, K. Ito, I. Ida, and M. Takahashi, "The SAR Evaluation Method by a Combination of Thermographic Experiments and Biological," IEEE Trans. Microw. Theory Tech., vol. 48, pp. 2094–2103, 2000.